J Electroceram (2006) 16: 35–39
DOI 10.1007/s10832-006-4351-7

Initiation of tantalum oxide pores grown on tantalum by potentiodynamic anodic oxidation

I. Sieber · H. Hildebrand · A. Friedrich · P. Schmuki

Received: April 22, 2005 / Revised: August 15, 2005 / Accepted: August 18, 2005
© Springer Science + Business Media, Inc. 2006

Abstract The initiation and growth of porous oxide on Ta was investigated in mixed H_2SO_4/HF electrolytes. Under selected potentiodynamic anodic oxidation conditions the formation of nearly uniform porous Ta_2O_5 layer was observed. The porous Ta_2O_5 layers consist of self-organized pore arrays with single pore diameters ranging from 2 to 10 nm. The morphology and the thickness of the layer depend strongly on the applied potential, the scan rate and on HF presence. The composition of the porous oxide layer is Ta_2O_5.

Keywords Porous tantalum oxide · Self-organization · Electrochemical oxidation · Potentiodynamic anodic oxidation

Introduction

Electrochemically grown pores in metals and semiconductors have been studied for about 50 years. However, only in the last 10–15 years intensive research efforts have enabled the preparation of ordered arrays of pores with pore diameters varying from few nanometers up to few tens of micrometers. The most studied material is porous alumina [1]. For other metals, e.g. Ti [2–6], Zr [7], Sn [8], Hf [9], Ta [10] and Nb [11], only a few recent reports are available, where successfully a highly ordered porous oxide structure has been produced.

Tantalum oxide has received considerable attention as a protective coating material for chemical equipment, as part of optical devices and as suitable material for storage capacitors in very large-scale integrated circuits [12–17]. Due to the excellent dielectric properties, the fabrication of porous Ta_2O_5 films with a large surface area and high specific charge seems to be promising for applications in electronic and sensor devices.

The anodization of tantalum has been intensively studied in various electrolytes (e.g. sulfuric acid, phosphoric acid and NaOH solutions) at voltage typically up to 200 V [18–20]. Under these electrolyte conditions, and if the potential is kept below the dielectric breakdown potential, a uniform layer of amorphous tantalum oxide is obtained [19, 20]. Most of the work focuses on the growth mechanism and the protective properties of the compact metal oxide under the influence of different parameters (e.g. temperature, nature of the electrolyte and its concentration) [14–22].

Up to now there are only few reports [23, 24] describing controlled electrochemical pores formation on tantalum at potentials below the breakdown potential. Own previous work [10] has shown that a highly assembled pore distribution is obtained in 1 M H_2SO_4 + 2 wt% HF with nano-sized pores, ranging from 15 to 20 nm. The pores appear to be randomly located but have a relatively narrow size distribution with a high degree of porosity extending in the depth.

The present work deals with a systematic investigation of the process of pore initiation depending on the scan rate and the anodic potentials.

Experimental

Material and surface preparation

The material used was Ta-foil (Goodfellow, 99.5%, thickness 0.1 mm). The surface of the specimens was cleaned ultrason-

I. Sieber (✉)· H. Hildebrand · A. Friedrich · P. Schmuki
University of Erlangen-Nuremberg, Department of Material Science, Chair for Surface Science and Corrosion, D-91058 Erlangen, Germany
e-mail: irina.sieber@ww.uni-erlangen.de

ically with ethanol, distilled water, and dried with in a stream of Ar. Experiments were performed in electrolyte with a composition of 1 M H_2SO_4 + 2 w.t.% HF. The solutions were prepared from reagent-grade chemicals and distilled water. All experiments were conducted at room temperature.

Electrochemical studies

A conventional electrochemical cell with three electrodes was used for electrochemical investigations. Platinum gauze served as a counter electrode. The electrode potential was measured with reference to Hg/$HgSO_4$ mercury-sulfate electrode (MSE) (with a potential of 0.680 V vs. NHE) and all data were reported in the mercury-sulfate electrode scale. The electrochemical treatment consisted of a potential ramp from the open-circuit potential (E_{OCP}) or to E_{end} = 10–20 V with a scan rate of 10–100 mV sec^{-1} using HI VOLTAGE potentiostat Jaissle IMP88PC-200V + PRODIS.

Anodic polarization curves were performed under potentiodynamic control (5–100 mV sec^{-1}) using ZAHNER potentiostat-galvanostat (IM6 12090).

Surface characterization

After cutting off the anodizing current, the specimens were taken out of the solution, quickly washed with distilled water and dried with Ar. Micrographs of the metal surface were provided by a HITACHI S4800 scanning electron microscope (SEM). Chemical characterization was carried out by X-ray photoelectron spectroscopy (XPS) using the Ta peak at 23 eV, the O peak at 528 eV, the *F* peak at 685 eV, and the S peak at 165 eV [25]. For quantitative analyses the element sensitivity factors provided by the manufacturer were used. Spectra were acquired on PHI 5600 XPS spectrometer. The oxide layer thickness was determined from XPS sputter profiles acquired by Ar^+ sputtering at 3.2 kV. The sputter rate was obtained from calibration with direct SEM cross-section thickness measurements provided for a 0.1 mm thick Ta-foil.

Results and discussion

Figure 1(a) shows the anodic polarization curves (APC) for Ta in H_2SO_4 and H_2SO_4 + 2 wt% HF electrolytes for different scan rates. In H_2SO_4 and in the potential range up to 2 V, Ta is stable and shows immediate metal passivation [21]. Under these conditions, the growth of a compact Ta_2O_5 film on the Ta anode is obtained [18, 19]. The current increase in the H_2SO_4 electrolyte in the potential region at 2–5 V is typically ascribed to oxygen formation and acidification [26].

In presence of HF the polarization behavior changes drastically. Clearly a general trend to higher current densities can be observed with increasing the scan rate value. In contact to H_2SO_4, the APCs in the HF electrolytes show a second broad peak in the range of 5–10 V and above. The current peak and the peak potential depend on the scan rate (Fig. 1(b) and (c)) and show exponential and linear dependence, correspondingly.

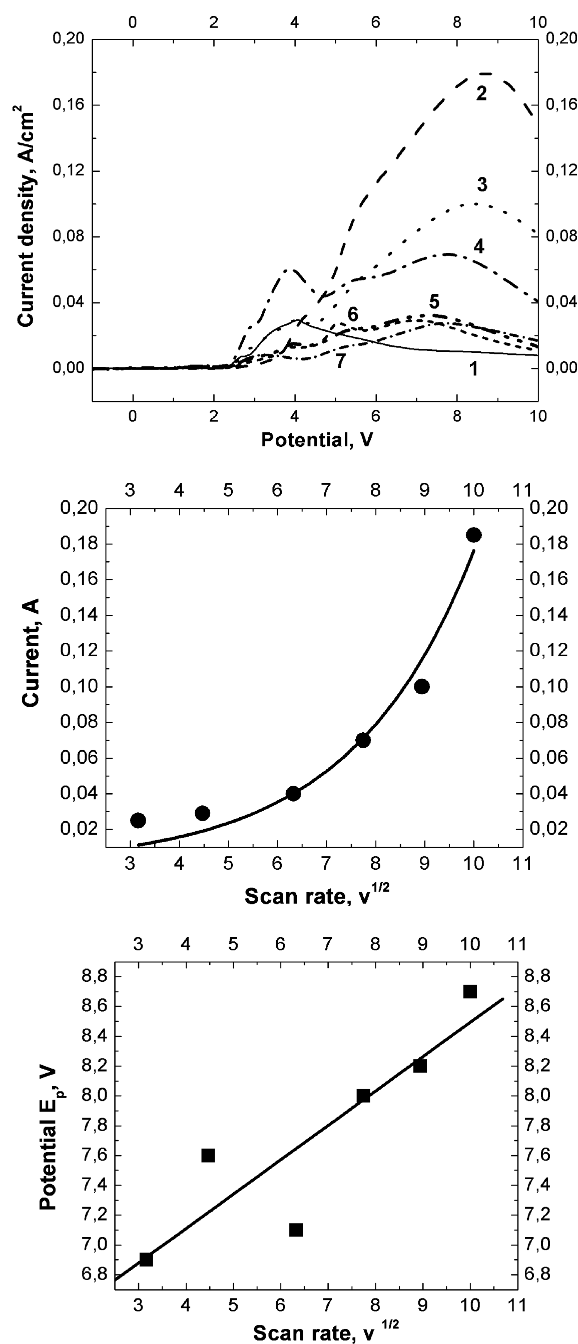

Fig. 1 Anodic polarization curves of Ta in 1 M H_2SO_4 (curve 1) and in 1 M H_2SO_4 + 2 wt% HF (curves 2–7) with a different scan rate: 1, 2–100 mV sec^{-1}; 3–80 mV sec^{-1}; 4–60 mV sec^{-1}; 5–40 mV sec^{-1}; 6–20 mV sec^{-1}; 7–10 mV sec^{-1} (a) and dependence of the peak current (b) and peak potential (c) versus the square root of the scan rate

Generally, the increase of the current density on the APCs can be associated with the dissolution of the anodic oxide layer, the formation of a new phase or a change in the attack morphology (pore formation/smoothing, changing the effective electrode area). Previous work [10] presented the assumption that the morphological change is due to a second peak maximum in the polarization behavior. However, the potential at which the process of pore nucleation starts could not yet determined.

In order to get information about Ta surface morphology, the samples after anodic oxidation till 10 V with a different scan rate (10–100 mV/sec) were examined with SEM. It was noted, that at 10 V and for APCs taken with a small scan rate, the second peak is not clearly detectable and current arrives at its steady state value very early.

SEM investigations show details of the pore initiation. In general, no effect of HF on the top view morphology can be formed for samples anodized with a scan rate of 100 mV/sec. Decreasing the scan rate to 80 mV/sec leads to the appearance some traces of HF attack (Fig. 2(a)), and at 40 mV/sec clear pore nucleation can be observed (Fig. 2(b)). Significant porosification of the surface oxide layers was found on several samples after decreasing the scan rate to 10 mV/sec (Fig. 2(c)). Obviously, the porous structure at 10 V is not homogeneously distributed across the surface. There are some larger pores possibly related to the process of gas evolution.

Evidently, the process of pore initiation is time dependent and a dynamic equilibrium between Ta_2O_5 formation/dissolution controls the time scale of the development of porosity and the ordering effects of the formed oxide layer.

Effect of scan rate on the form of APCs can be explained as a change in the attack morphology (pore formation, changing the effective electrode area). Also, the non-linear dependence of the peak current versus scan rate root (Fig. 1(b)) looks not surprising as a result of the non-continuous porous layer formation with different porosity. The appearance of a current maximum on the APCs is typical for pore formation process. Due to the solubility of the metal oxide in HF-containing solutions, first pores start to grow randomly and the current increases (due to a surface area increase) until a competition between the growing pores takes place. If a steady pore growth situation can be established the current drops to a trans-passive value corresponding to the dissolution rate at the pore front. Obviously for the system with a smaller scan rate pore growth is possible already at potentials closed to trans-passive value, for the system with a higher scan rate pore formation is available only at higher potentials (Fig. 1(c)).

In order to check influence of the anodic potential value on the Ta porous structure developing, the surface of Ta samples were analyzed with SEM after anodic oxidation the samples to different values of anodization end potentials (10–20 V) (Figs. 2(c) and 3(a), (b)). In general, increasing potential

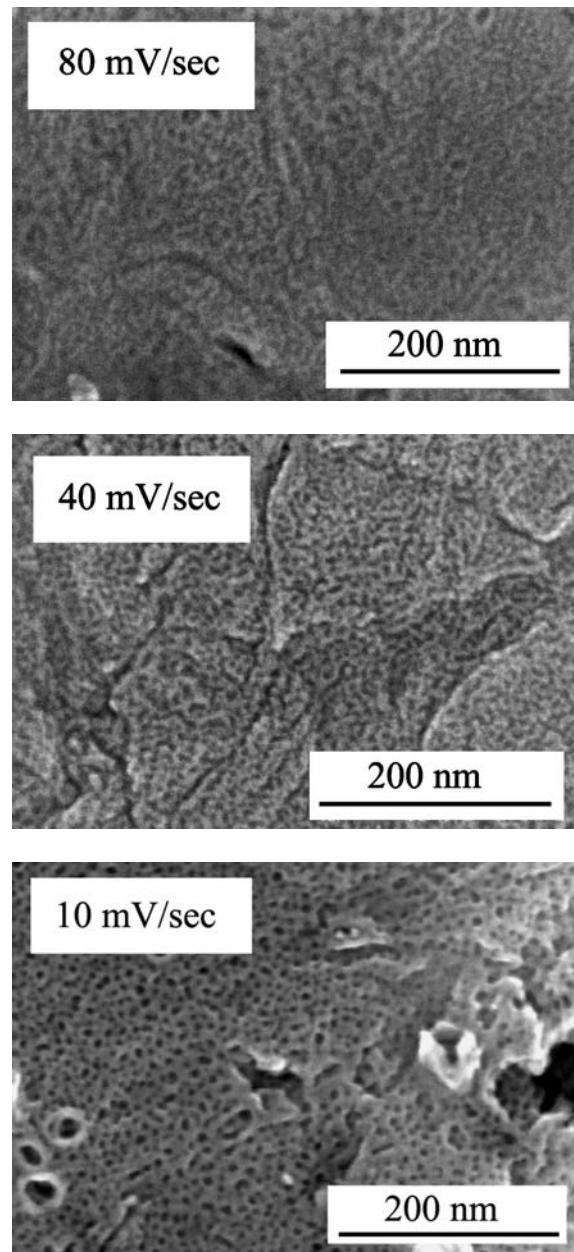

Fig. 2 SEM images of Ta anodized from E_{OCP} till 10 V with different scan rate in 1 M H_2SO_4 + 2 wt% HF: (a) 80 mV sec^{-1}, (b) 40 mV sec^{-1}, (c) 10 mV sec^{-1}

to 20 V leads to an uniform porous distribution across the surface and an increasing the pore diameter from 2 to 10 nm.

In order to gain information on the composition of formed films after anodic polarization in 1 M H_2SO_4 and in 1 M H_2SO_4 + 2 wt% HF and on the distribution of elements inside the films, XPS sputter profiles were acquired. The films in all cases showed a composition corresponding to Ta_2O_5. Some traces of F (from HF) could be detected throughout the film whereas S (from the electrolyte SO_4^{2-}) was not detected. The thicknesses of a compact layer formed in H_2SO_4

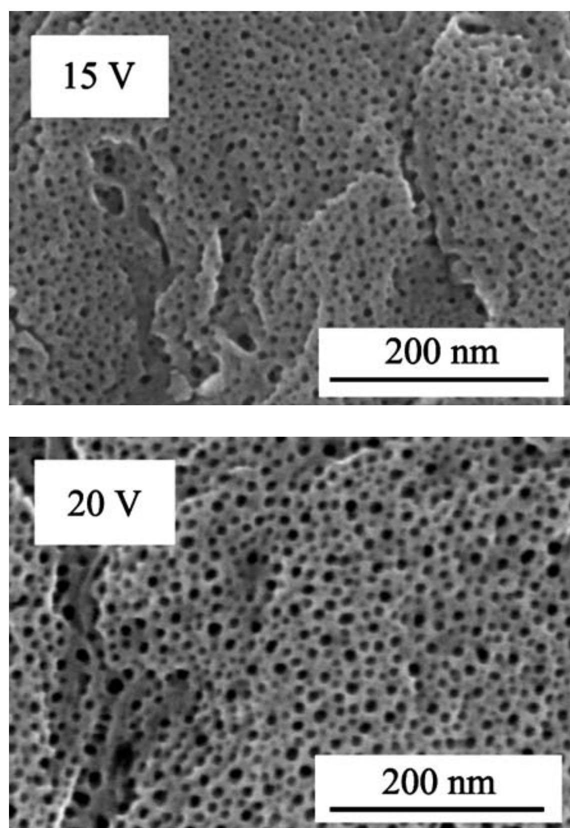

Fig. 3 SEM images of Ta anodized from E_{OCP} to 15 (a) and 20 V (b) in 1 M H_2SO_4 + 2 wt% HF (scan rate is 10 mV sec^{-1})

is 32 nm whereas the porous layer formed in a HF containing electrolyte at 20 V results as 130 nm (Fig. 4).

It is well known [18, 19], that the growth of tantalum oxide is generated by high-field ionic transport process, associated with the migration of tantalum and oxygen ions. An anion transport number of around 0.5 (Ta) leads to oxide formation at both interfaces, e.g., at the metal/oxide interface by Ta^{5+} transport and at the oxide/electrolyte interface by oxygen transport. As a result, oxide films thicken linearly with an increase of the electrode potential (1.6 nmV^{-1}) [14–22] and at 20 V correspond to 32 nm. Previous work often found a thickening of oxide layers in HF containing electrolytes. This was ascribed to an assumption that in HF containing electrolytes, during anodic oxidation of tantalum, fluoride ions move inward with an average mobility that is 1.85 faster that of oxygen ions; and that this mobility is independent of film thickness [27, 28]. As a direct consequence of the increased mobility of fluoride ions compared with oxygen ions, is the thickening of the porous Ta_2O_5 layer in comparison with a layer produced in F free electrolyte (from 32 to 130 nm). It was suggested [28] that the migration of fluoride ions is closely correlated with the migrations of tantalum and oxygen ions during high field anodic oxidation of tantalum. It could be agreed that this process is an ill-defined process of

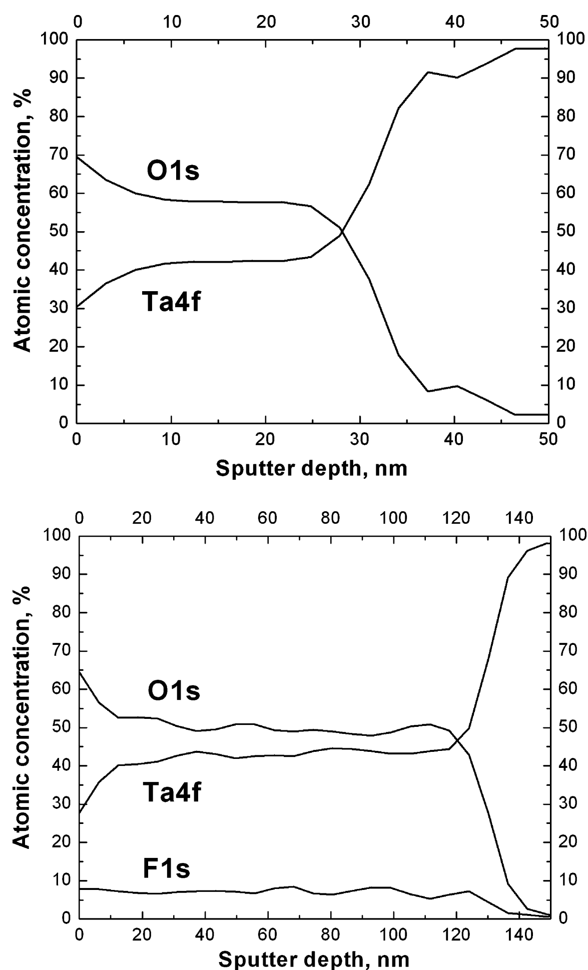

Fig. 4 XPS depth profile of the main elements in the compact (a) and pores (b) oxide film derived from the Ta which had been anodized at 20 V in 1 M H_2SO_4 (a) and in 1 M H_2SO_4 + 2 wt% HF (b) electrolytes

ionic transport involved in the anodic oxide growth on Ta. An absence of the linear dependence of the peak current versus scan rate roots (Fig. 1(b)) would directly supplied this proposal. Because for processes with transport control the linear dependence of the peak current versus scan rate roots is normally expected. However the present work shows clearly that thickening is due to pore formation process. Whether or not fluoride migration through the oxide plays a key role in this process can not unambiguously be decided. From a practical view point the work shows clearly pathways to tailor the morphology of self-organized porous Ta_2O_5 by electrochemical parameters.

Conclusions

The work investigates factors affecting the process of self-assembled pore initiation and growth on tantalum. It is evident that nearly uniform porous tantalum oxide layer can

be formed with pore diameters in the range of 2 to 10 nm. The process of pore initiation is dependent on several electrochemical factors. A dynamic equilibrium between Ta_2O_5 formation and dissolution controls the time scale for the initiation and development of the morphology of the pores. The same factors also affect the ordering of the formed oxide layer.

Acknowledgments The authors acknowledge the Deutsch-Französische Hochschule for organization and supporting the first German-French Summer School on Electrochemistry and Nanotechnology and the University of Erlangen-Nuremberg, University of Provence, CNRS, Metrohm, Autolab and Raith for their financial contributions.

References

1. H. Masuda and K. Fukuda, *Science*, **268**, 1466 (1995).
2. V. Zwilling, M. Aucouturier, and E. Darque-Ceretti, *Electrochim. Acta*, **35**, 921 (1999).
3. D. Gong, C.A. Grimes, O.K. Varghese, W. Hu, R.S. Singh, Z. Chen, and E.C. Dickey, *J. Mater. Res.*, **16**, 3331 (2001).
4. T. Oishi, T. Matsurbara, and A. Katagiri, *Electrochemistry*, **68**, 106 (2001).
5. R. Beranek, H. Hildebrand, and P. Schmuki, *Electrochem. Solid-State Lett.*, **6**, B12, (2003).
6. J.M. Macak, K. Sirotna, and P. Schmuki, *Electrochim. Acta*, (2004) in press.
7. H. Tsuchiya and P. Schmuki, *Electrochem. Commun.*, **6**, 1131 (2004).
8. H.-C. Shin, J. Dong, and M. Liu, *Adv. Mater.*, **16**, 237 (2004).
9. H. Tsuchiya and P. Schmuki, *Electrochem. Commun.*, **7**, 49 (2005).
10. I.V. Sieber, B. Kannan, and P. Schmuki, *Electrochem. Solid-State Lett.*, **8**, J10 (2005).
11. I.V. Sieber, H. Hildebrand, A. Friedrich, and P. Schmuki, *Electrochem. Commun.*, **7**, 97 (2005).
12. Y. Masuda, S. Wakamatsu, and K. Koumoto, *J. Europ. Ceramic Soc.*, **24**, 301 (2004).
13. K. Kamada, M. Mukai, and Y. Matsumoto, *Electrochim. Acta*, **49**, 321 (2004).
14. A. Mozalev, M. Sakairi, I.Saeki, and H. Takahashi, *Electrochim. Acta*, **48**, 3155 (2003).
15. A.I. Vorobyova and E.A. Outkina, *The Solid Films*, **324**, 1 (1998).
16. W.S. Kim, J.H. Kim, J.H. Kim, K.H. Hur, and J.Y. Lee, *Materials Chemistry*, **79**, 204 (2003).
17. C. Wang, L. Fang, G. Zhang, D-M. Zhuang, and M.-S. Wu, *Thin Solid Films* (2003), in press.
18. Q. Lu, S. Mato, P. Skeldon, G.E. Thompson, D. Masheder, H. Habazaki, and K. Shimizu, *Electrochim. Acta*, **47**, 2761 (2002).
19. L. Young, *Anodic Oxide Films*, (Academic Press, London, 1961).
20. D.A. Vermilyea, *Acta Metallurgica*, **1**, 282 (1953).
21. J.W. Schultze, M. Pilaski, M.M. Lohrengel, and U.König, *Faraday Discuss.*, **121**, 211 (2002).
22. T. Hurlen and E. Gulbranden, *Electrochim. Acta*, **39**, 2169 (1994).
23. Q. Lu, G. Alcala, P. Skeldon, G.E. Thompson, K. Shimizu, and H. Habazaki, *Electrochim Acta*, **48**, 37 (2002).
24. Q. Lu, P. Skeldon, G.E. Thompson, M.J. Graham, M. Dasheder, H. Habazaki, and K. Shimizu, *J. Electrochem. Soc.*, **149**, B 531 (2002).
25. Handbook of X-ray Photoelectron Spectroscopy, By J. F. Moulder, W. Stikle, Published by Physical Electronics, Minnesota, 1995.
26. M. Pourbaix, Atlas of Electrochemical Equilibria in Aqueous Solutions, 1974.
27. R.E. Pawel, J.P. Pemsler, and C.A. Evans, *J. Electrochem. Soc.*, **119**, 24 (1972).
28. K. Shimizu, K. Kobayashi, G.E. Thompson, P. Skeldon, and G.C. Wood, *J. Electrochem. Soc.*, **144**, 418 (1997).